Radio Science, Volume 20, Number 3, Pages 643–651, May–June 1985

Ionospheric scintillation measurements at 1.5 GHz in mid-latitude region

Yoshio Karasawa, Koji Yasukawa, and Matsuichi Yamada

Research and Development Laboratories, Kokusai Denshin Denwa Co., Ltd., Tokyo, Japan

(Received May 8, 1984; revised September 7, 1984; accepted September 21, 1984.)

Anomalous signal fluctuations due to ionospheric scintillation at 1.5 GHz appear occasionally on earth-space paths in maritime satellite communication. With regard to the characteristics of ionospheric scintillations at gigahertz frequencies, few data are available in the middle latitude region. This paper describes the results of 1.5-GHz scintillation measurements at Yamaguchi, Japan. Measurements were carried out by receiving a 1.5-GHz beacon signal from the MARISAT satellite over the Indian Ocean with an elevation angle of 17.3°. In 13 months of measurements, very severe scintillation with peak-to-peak fluctuations exceeding 30 dB was observed in the equinoctial month, and a number of spike-type scintillations were also observed, particularly at night. Scintillation characteristics, such as diurnal and seasonal variations, amplitude distribution, spectrum, and depolarization are discussed.

1. INTRODUCTION

In existing maritime satellite communication systems organized by the International Maritime Satellite Organization (Inmarsat), *L* band (uplink: 1.6 GHz; downlink: 1.5 GHz) circularly polarized waves have been used in all satellite-to-ship links, and partly in satellite-to-CES (Coast Earth Station) links for automatic frequency control (AFC) purposes. On these *L* band links, anomalous signal fluctuations due to ionospheric scintillations appear occasionally in addition to tropospheric scintillations. Especially after a geomagnetic storm has occurred in the ionosphere, very large scintillations of magnitudes exceeding 20 $dB_{p\text{-}p}$ (peak-to-peak) are likely to occur, during which time, system performance of maritime satellite communication is degraded. Therefore, it is crucial that the effects of *L* band ionospheric scintillation be made clear.

With regard to characteristics of ionospheric scintillations at gigahertz band frequencies, a large number of studies have been performed from experimental and theoretical points of view mainly in the last decade [*Taur*, 1973, 1976; *Basu et al.*, 1976; *Crane*, 1977; *Yeh and Liu*, 1982; *Aarons*, 1982; *Fang and Liu*, 1983]. Through the continuous efforts of various investigators, global morphology and qualitative characteristics of gigahertz band scintillation have gradually been made clear, particularly in equatorial and polar regions. Based on much data collected in American, European and African regions, studies have revealed that ionospheric scintillation is caused by electron density irregularities generated in the ionospheric *F* region (such as spread *F*) or *E* region (sporadic *E*), and that the frequency distribution of scintillation occurrence has a fairly large dependence not only on the geomagnetic latitude but also on the longitude [*Basu et al.*, 1976]. However, a few data available at *L* band frequencies in the Asian region [*Fujita et al.*, 1978; *Moriya and Sakurada*, 1983] were still insufficient for quantitative studies on mid-latitude scintillations.

In order to establish a reliable data base for designing *L* band satellite communication systems, we have carried out scintillation measurements since April 1982 at the Yamaguchi Satellite Communication Center (131°33′E, 34°12′N) in Japan by receiving an *L* band beacon signal (1541.5 MHz, right-handed circular polarization (RHCP)) transmitted from the MARISAT satellite at 73°E over the Indian Ocean. In this paper, we present the results of 13 months of observations on 1.5 GHz ionospheric scintillations. The discussion mainly emphasizes on spike-tupe scintillation, diurnal and seasonal variations of scintillation occurrence, power spectrum of Rayleigh-type fluctuations, and depolarization of circularly polarized waves during scintillation.

2. OUTLINE OF EXPERIMENT

Figure 1 shows the path geometry between Yamaguchi and the MARISAT satellite at 73°E over the Indian Ocean, with a path elevation angle of 17.3°.

Paper number 4S1239.
0048-6604/85/004S-1239$08.00

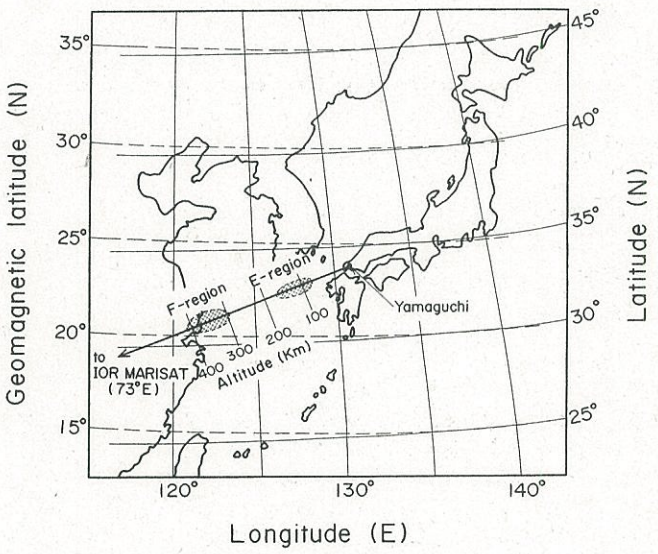

Fig. 1. Geometry of propagation path.

The propagation path penetrates the ionospheric *F* region (altitude assumed to be 300–400 Km) over Shanghai, and also penetrates the *E* region (90–120 Km) over the ocean near the Korean Peninsula. These areas are depicted by shading in Figure 1. Since their geomagnetic latitudes range from 20° to 25°, scintillations observed at Yamaguchi seem to be mid-latitude yet having a partially equatorial nature. The crossing angle between the propagation path at the ionospheric *F* region and geomagnetic field is about 64°. Polarization of received 1.5 GHz signals was slightly elliptical with an axial ratio of 2.8 dB. System parameters and configurations of the measuring system are summarized in Table 1.

A cross-dipole fed paraboloidal antenna (4 m in diameter) was used for receiving, and each component of the cross-dipole was individually used so as to measure both amplitudes of horizontal and vertical polarization components and their phase difference. Depolarization characteristics of received signals could be easily determined by using the above-mentioned three measured values. The noise figure of the receiving system was 1.8 dB and the normal receiving level was 35 dB higher than threshold level of the receiver. Figure 2 shows a block diagram of the measuring system. The *L* band receiver was composed of an RF section equipped just behind the antenna and an IF/Detector section installed in a separate room. In order to eliminate errors due to system gain drifting and phase fluctuation caused by variations in ambient temperature during the long observation period, sequential automatic system calibration was employed, as shown in Figure 2. This calibration was performed by switching input ports of dual low noise amplifiers (LNA's) from the received signal to reference signal of the same frequency at a time interval. All data collected in experiments were recorded on a strip chart and magnetic tape.

The equivalent isotropic radiation power (EIRP) of the 1.5 GHz beacon signal transmitted from the Marisat satellite decreases with increasing traffic loads (telephone calls) due to the nonlinearity of satellite *L* band high power amplifier (HPA). However, this influence can be excluded easily by utilizing the inherent nature of the changing pattern of the signal level such that the signal level changes discretely with a constant value just after telephone calls have started (or finished).

3. EXPERIMENTAL RESULTS AND DISCUSSIONS

3.1. *Scintillation patterns*

Anomalous signal fluctuations with various patterns were sometimes observed mainly at nighttime. The occurrence time and magnitude of these fluctuations had no correlation with those of the 11 GHz band tropospheric scintillation simultaneously observed at the same site whose azimuth was nearly the same at an elevation angle of 6.5° [*Karasawa and Yasukawa*, 1983]. Judging from these facts, it can be concluded that the fluctuations are due to the ionospheric effect caused by electron density irregularities in the ionospheric *F* or *E* region.

Scintillations recorded on strip charts can be classified into two typical patterns. One type is

TABLE 1. Parameters of Measurement System

Received Signal, 1.5-GHz Beacon From the Marisat Satellite Located at 73°E	Frequency	1541.5 MHz
	Polarization	RHCP,
	Axial Ratio (Measured)	2.8 dB
Antenna	type	4 m paraboloidal
	gain	31.4 dB
	axial ratio	0.8 dB
Receiver	noise figure	1.8 dB
	threshold level	−175 dBW
	normal signal level	−140 dBW
Measured items	(1) amplitude of horizontal polarization component: $\lvert E_H \rvert$	
	(2) amplitude of vertical polarization component: $\lvert E_V \rvert$	
	(3) phase difference between E_H and E_V	
Elevation angle	17.3°	
Measurement period	April 29, 1982, to May 26, 1983	

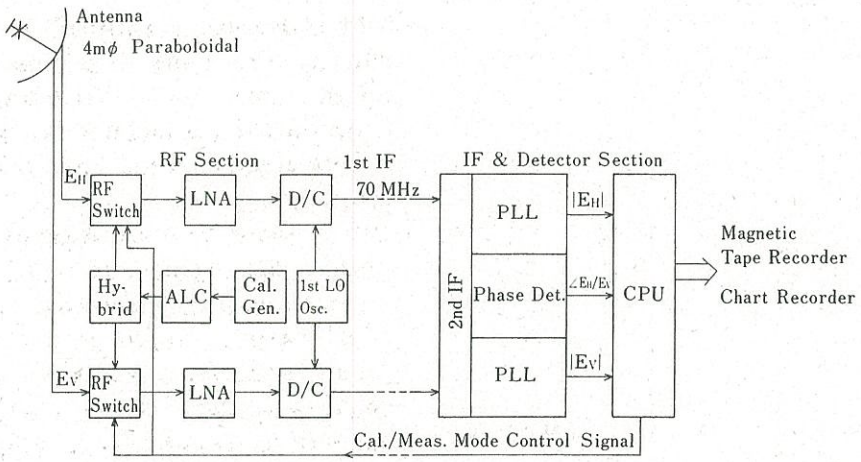

Fig. 2. Block diagram of receiving system:

[LNA: low noise amplifier, D/C: down converter
ALC: automatic level control, Cal Gen: calibration signal generator, PLL: phase locked loop]

characterized by rapidly increasing fluctuations at the initial stage and gradually diminishing fluctuations at the final stage as shown in Figure 3. This fluctuation pattern is commonly seen in literatures on ionospheric scintillations and is hereafter called "type C." The other is spike-type (or impulsive) fluctuation as shown in Figures 4*a* and 4*b*, hereafter called "type S."

As for the scintillation of type C, it is well known that the cause of the occurrence is closely connected with the spread *F* at nighttime and the sporadic *E* in the daytime [*Aarons and Whitney*, 1968; *Fujita et al.*, 1978]. On the other hand, interpretations of type S scintillation seem to be scarcely given as far as we know, though the same type of fluctuation was reported by *Moriya and Sakurada* [1983] through 1.5 GHz measurements. Accordingly, we will focus our discussions on the type S scintillation in the next section.

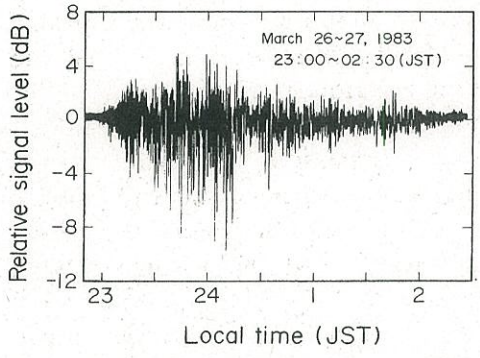

Fig. 3. Typical pattern of "type C" scintillation.

3.2. *Spike-type scintillation*

In some cases, a number of spike-type fluctuations occurred in succession one night, as shown in Figure 4*a*, and, in some cases, only one appeared at night. It

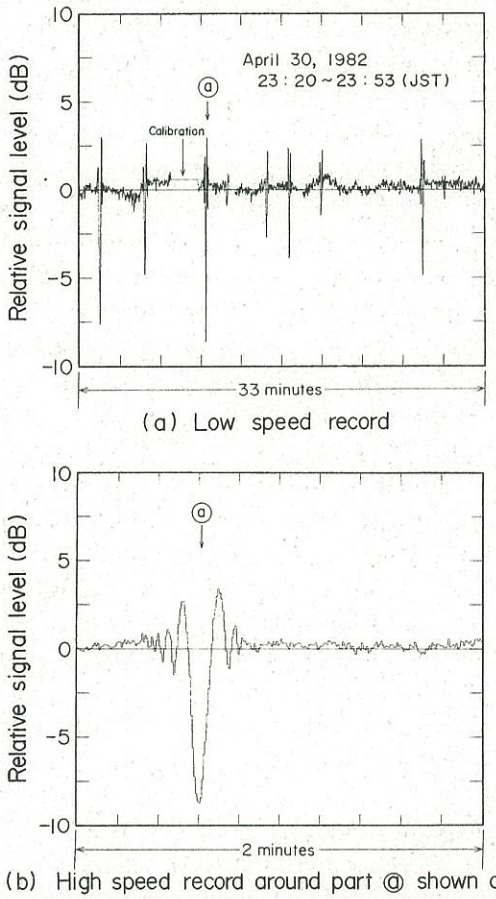

Fig. 4. Typical pattern of "type S" scintillation. (*a*) Low speed record. (*b*) High speed record around part a shown above.

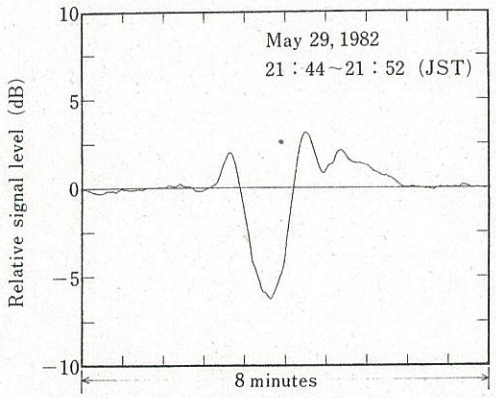

Fig. 5. "Type S" scintillation lasting for an extended period.

is worthy to note that the shape of almost all the type S scintillations was symmetrical with a deep central minimum in the time domain, as shown in Figure 4*b*. The maximum fade during the 13-month-long observations was 12 dB lower than the normal level, and the period between two enhanced peaks was widely distributed ranging from 5 s to 2 min. An example with a long duration period is shown in Figure 5.

In general, similar fluctuations can occur in the following cases: (1) fluctuation of satellite EIRP itself, (2) ambient noise or interference, (3) troubles in the receiving system, (4) reflection or blockage by a vehicle such as an airplane or a helicopter, (5) diffraction due to a meteor trail generated in the ionospheric *E* region, or (6) tropospheric effects, such as scintillation or attenuation. Therefore, careful examination is needed before this spike-type fluctuation can be identified as ionospheric scintillation.

We will now examine each item mentioned above. (1) According to simultaneous observations of the same satellite signal at two long-distant sites [*Moriya and Sakurada*, 1983], no time-to-time correspondence as to the occurrence time of spike-type fluctuations could be seen although the same statistical features regarding its occurrence time were found. (2) If the signal is affected by ambient noise or interference, a fairly large cross-polarization component must be observed. However, the cross-polarization component even in the case of 12 dB fade (to be shown in section 3.6) was not larger than −30 dB. (3) The same statistical characteristics as to occurrence time and occurrence season were observed at three independent receiving sites (Yamaguchi, Hiratsuka, and Miyakonojo [*Moriya and Sakurada*, 1983]). (4) Judging from the speed of flying vehicles such as airplane or helicopters, the duration of the fluctuation should be smaller than 1 s in the case of passing through primary Fresnel regions of the wave path, making it difficult to explain the fact that measured durations ranged from 5 s to 2 min. Additionally in the case of reflection from a metallic body, such as an airplane or helicopter, a large magnitude cross-polarization component must be recorded because circularly polarized waves having an opposite sense of rotation come to the antenna. However, the observed cross-polarization component was negligibly small as mentioned above. Moreover, the Yamaguchi Satellite Communication Center is carefully protected from the effects of airplane operation. (5) It is well known that meteor trails are mainly produced around 0600 hours in the morning, while the occurrence time of the spike-type fluctuations were concentrated around 2000–2400 hours. (6) We could not find such spike-type fluctuation in the simultaneous tropospheric scintillation measurements at 11 GHz with an elevation angle of 6° and nearly the same azimuth as the 1.5 GHz measurements.

In light of this, what is the cause of spike-type fluctuations? For the frequencies lower than 1 GHz, impulsive (or spike-type) fluctuations similar to our "type S" scintillations can be seen in some papers [*Slack*, 1972; *Davies and Whitehead*, 1977; *Hajkowicz et al.*, 1981] as called by "quasi-periodic (QP) scintillations." Since the impulsive fluctuations reported so far including our experiments were mostly appeared in the middle latitude regions, origin of such fluctuations may have strong dependence on the latitude.

Considering the shape of fluctuations, it is likely that the spike-type fluctuations have a connection with small-scale irregularities generated in the ionosphere. One probable solution of their origin is due to the diffraction or interference caused by ionospheric bubbles or blobs. However, scintillations caused by bubbles are characterized by the signal increase at the center of the fluctuation pattern [*Tyagi et al.*, 1982] because the ionization inside the bubble is depleted. Therefore, the fluctuation pattern caused by the bubbles is upside down in our case as shown in Figure 4. Moreover, the bubbles are mainly produced in equatorial regions and it may be not appropriate in the middle latitude regions. On the other hand, it is possible to explain our results by introducing the lens effect caused by blobs, in which ionization is enhanced [*Davies and Whitehead*, 1977].

Although we cannot make sure in what region (namely, ionospheric *F* or *E* region) the type S scintillations were generated, type S scintillations may have deep connection with irregularities in the ionospheric *F* region because they correlated very well with the

generation of the type C night time scintillations to be shown in the next section. Anyhow, observations of spike-type scintillations at frequencies other than *L* band and at other sites are quite important to clarify small-scale irregularities in the ionosphere.

3.3. *Frequency distribution of occurrence*

Figure 6 shows a histogram of onset time of scintillations classified by type C and type S. In this data analysis, we define onset time as the time when peak-to-peak fluctuation exceeds 2 dB in the initial stage of a scintillation. In the case that a number of type S scintillations appear successively within one hour, we count only the first one among them. As can be seen in this figure, two notable peaks appear around 0900–1500 hours during the day and 2000–0100 hours at night. As far as type S scintillations are concerned, most of them could be seen at night. Based on previous studies [*Aarons and Whitney*, 1968; *Fujita et al.*, 1978], nighttime scintillations are related to electron density irregularities in the ionospheric *F* region, while daytime scintillations have a strong connection with the effect of the ionospheric *E* region.

Figure 7 shows a seasonal variation of occurrences of scintillations classified by type for 13 months from May 1982 to May 1983. Data analysis was performed according to the same definition of scintillation occurrence mentioned above. Although the observation period was limited, the results indicate that scintillations occurred frequently in early summer, while few scintillations appeared in winter. The diurnal and seasonal variations described here agree well with the results obtained by *Fujita et al.* [1978], the experiments of which were carried out by observing 1.7 GHz satellite signal with an elevation angle of 47°. Considering the results obtained, there seems to

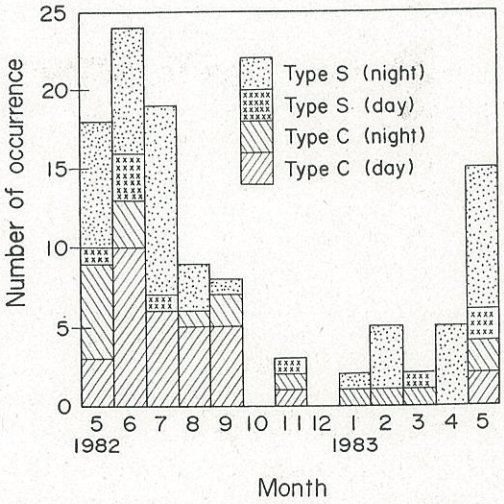

Fig. 7. Seasonal variation of "type C" and "type S" scintillations.

be a common feature having a single peak of percent occurrence around June in mid-latitude East Asian regions. On the other hand, scintillation activities are generally high during the equinoctial months in equatorial regions, as a matter of course, including Asian regions [*Fang and Liu*, 1983]. Although the season with high scintillation activity in mid-latitude regions is different from that in equatorial regions, the highest activity appears commonly in the season with the highest elevation angle of the sun in both regions. It may be true that the percentage occurrence of the scintillation will be in proportion to the ionization by the sun.

Figure 8 also shows seasonal variation of occurrences of scintillations classified according to the scintillation index SI defined as follow:

$$\mathrm{SI} = P_{\max} - P_{\min} \quad \mathrm{dB} \tag{1}$$

where $P_{\max}$ is the signal intensity of the third peak

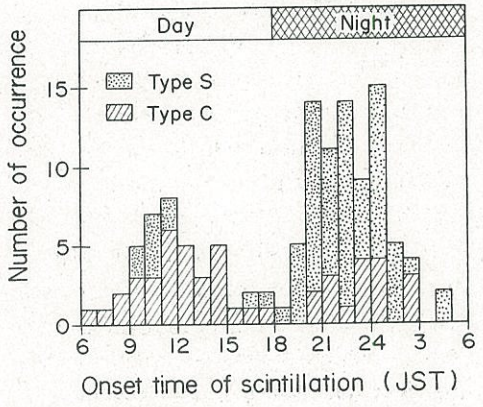

Fig. 6. Diurnal variation of onset time.

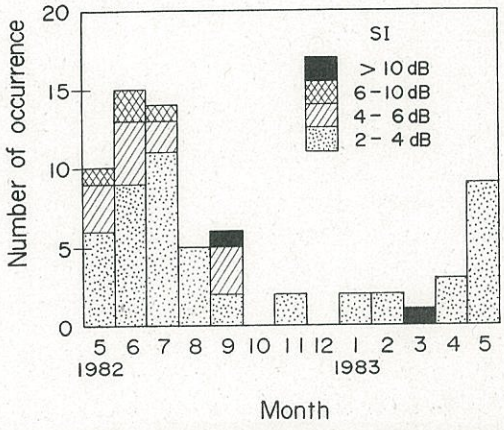

Fig. 8. Seasonal variation classified by scintillation index.

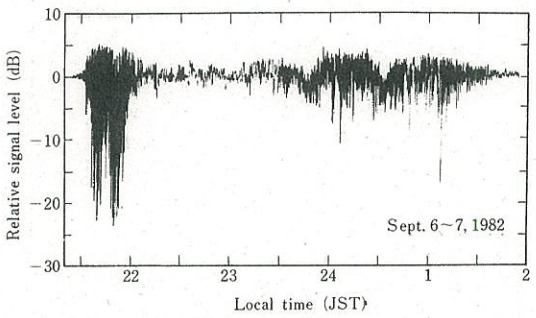

Fig. 9. Most significant scintillation occurring on Sept. 6–7, 1982.

down from the maximum excursion of the scintillation and P_{min} is the intensity of the third peak up from the minimum excursion measured in decibels. When this definition is employed, almost no type S scintillations are included in Figure 8. During 13-month-long observations, very severe scintillations whose scintillation index (SI) exceeded 10 dB occurred twice, once on Sept. 6, 1982, and the other on March 26, 1983. Figure 9 shows a record of the former event. As seen in this figure, intense fluctuation started suddenly at 2130 hours (JST) after a geomagnetic storm had occurred during that day. This scintillation was the largest one during the observation period, more than 30 dB_{p-p} signal fluctuations were recorded for about 30 min and the duration time of scintillations whose peak-to-peak fluctuation exceeded 2 dB amounted to about 4 hours. It can be concluded that a number of weak scintillations appear in early summer while strong scintillations are likely to occur in equinoctial months.

Figure 10 shows the cumulative time distribution of peak-to-peak fluctuations (dB_{p-p}) for type C scintillations through the entire observation period. In this analysis, peak-to-peak value is defined as the difference between the maximum and minimum levels every 2 min, the duration time of which is long enough to have sufficient peaks and short enough to keep a statistical steady state of fluctuation intensity. It is worthy to note that the effect of 1.5-GHz ionospheric scintillation over a time percentage smaller than 0.01% will be quite significant even in the mid-latitude region where scintillation activity is generally said to be weak.

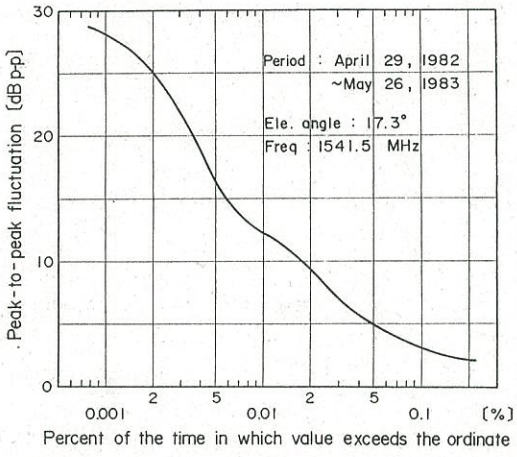

Fig. 10. Cumulative time distribution of peak-to-peak fluctuations throughout 13-month-long observations.

3.4. *Probability density function of fluctuation*

According to scintillation models developed by *Rufenach* [1975], the ionosphere acts as a screen that mainly changes the phase of waves passing through the slab. After emerging from the ionosphere, phase-disturbed waves turn gradually to amplitude-modulated waves with propagation along their paths due to the diffraction effect, and finally, the wave at a point sufficiently far from the ionosphere can be regarded as the sum of a coherent component (unperturbed field) E_C and an incoherent component (perturbed field) E_I. In this case, the amplitude of the coherent component and rms value of the incoherent component are respectively given by the following equations:

$$E_C = E_0 \exp(-\phi_0^2/2) \tag{2a}$$

$$(E_I)_{rms} = E_0(1 - \exp(-\phi_0^2))^{1/2} \tag{2b}$$

where E_0 is an incident signal level, and ϕ_0 is an rms value of phase fluctuation just after passing through ionospheric irregularities. Based on the above mentioned discussion, theoretical probability density

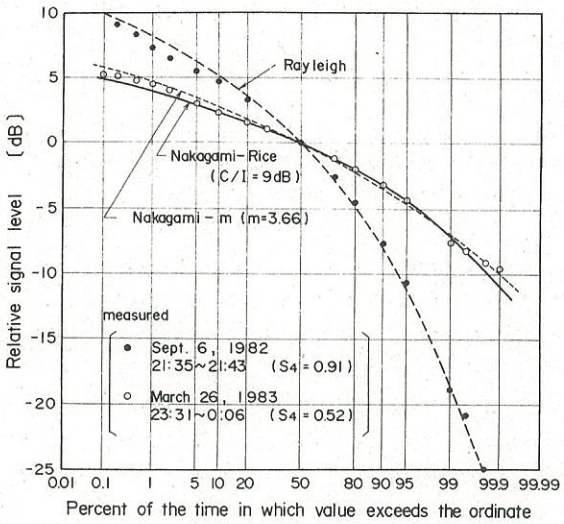

Fig. 11. Cumulative time distribution of amplitude during scintillation.

function (hereafter denoted as PDF) of ionospheric scintillation approximately results in the Nakagami-Rice distribution. On the other hand, it is well known that PDF of the ionospheric scintillations follows the nakagami-*m* distribution [*Crane*, 1977; *Yeh and Liu*, 1982]. Moreover, carefull examinations regarding the statistics of signal level variations of scintillations were performed comparing various PDF's such as the nakagami-*m*, lognormal, generalized Gaussian and two-component model by *Fremouw et al.* [1980], and results also indicate that the nakagami-*m* is the best fit PDF among them. Since the Nakagami-Rice distribution is somewhat similar to the Nakagami-*m* distribution for $m \geq 1$, discussion on the comparative merits between the Nakagami-*m* and Nakagami-Rice has no significance from a practical point of view. However, it seems to be better to identify the PDF of ionospheric scintillation with the Nakagami-Rice distribution for the purpose of better understanding of the physical meaning.

Figure 11 shows two examples of the cumulative time distribution of observed signal amplitudes. In this figure, the one for the largest scintillation occurring on Sept. 6, 1982 (pattern shown in Figure 9) is indicated by black dots and the other for the scintillation occurring on March 26, 1983 (pattern shown in Figure 3) is indicated by open circles. The former case, whose scintillation index S_4 amounted to 0.91, is very close to the Rayleigh distribution as depicted by a dashed line in Figure 11. It is interesting that the Rayleigh fading can occur even at gigahertz frequencies. The Nakagami-Rice and Nakagami-*m* distributions corresponding to the scintillation of the latter case are also shown by solid and broken lines, respectively. Both curves agree fairly well with measured data.

3.5. *Spectrum*

Figure 12 shows two spectra of the scintillation occurring on Sept. 6–7, 1982. Curve a represents a spectrum at an initial stage of very strong scintillation whose peak-to-peak fluctuations exceeded 30 dB, while curve b represents a spectrum at a final stage of the same scintillation whose peak-to-peak fluctuations ranged from 10 dB to 15 dB. According to the weak scintillation theory [*Rufenach*, 1975], roll-off part of scintillation spectrum follows the power law form of "f^n (f = spectral frequency)." A large number of spectra obtained so far have made clear the value of n ranging from -3 to -5 [*Crane*, 1977; *Basu et al.*, 1983]. Moreover, exact discussions

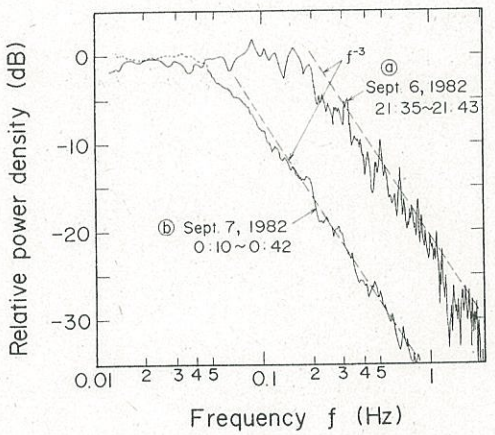

Fig. 12. Spectra of ionospheric scintillation.

on scintillation spectrum were made by *Franke and Liu* [1983] by introducing the two-component model. As can be seen in Figure 12, marked power law spectra with the form of f^{-3} were obtained for severe scintillations in our experiments. Observing 4-GHz equatorial scintillations, *Karasawa and Yasukawa* [1981] showed that the dominant period of fluctuating signal level during severe scintillations becomes longer gradually with increasing time, keeping the power-law form spectrum. Since we can also see the above mentioned phenomena in Figure 12, gradual change of power spectrum during scintillation seems to be a feature of severe ionospheric scintillations. Observed roll-off frequencies of each spectrum including other events were largely scattered from 0.02 Hz to 0.2 Hz.

3.6. *Depolarization*

As mentioned in section 2, depolarization characteristics of the 1.5-GHz wave can be obtained by using three measured values, namely, each amplitude of the horizontally polarized component ($|E_H|$) and vertically polarized component ($|E_V|$) and the phase difference between the two orthogonal components.

It is well known that the ionosphere acts as an anisotropic medium under the existence of geomagnetic field. Therefore, polarization of wave would be more or less distorted through ionospheric propagation. Since the quasi-longitudinal approximation is valid almost for any propagation angle relative to the earth's magnetic field at a frequency as high as 1.5 GHz, depolarization effects for right-handed circular polarization (RHCP) wave, which is one of the characteristics waves, are expected to be minimal. In the case of RHCP wave, generation of cross-polarization component (namely, left-handed circular

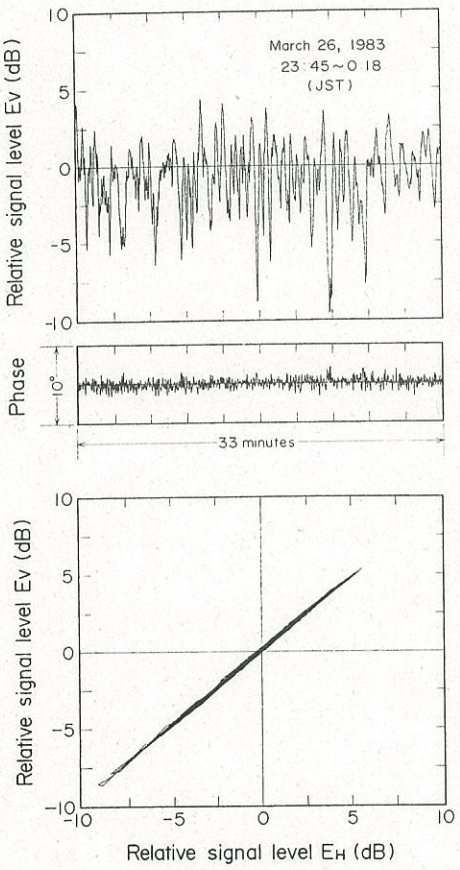

Fig. 13*a*

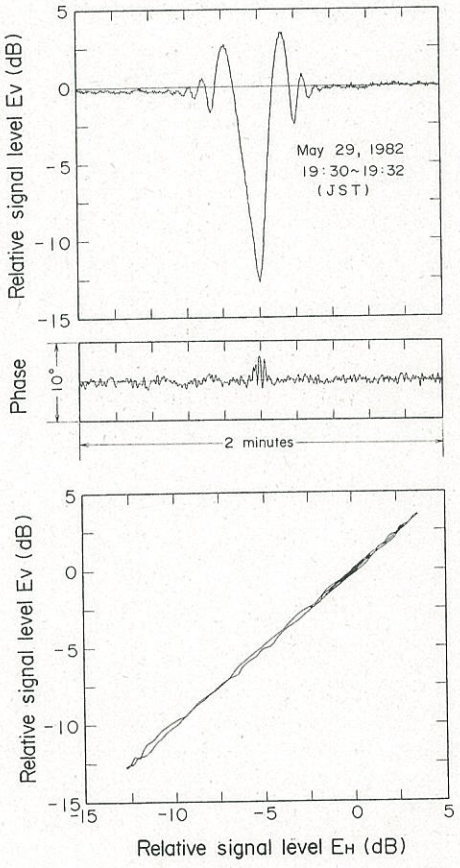

Fig. 13*b*

Fig. 13. Depolarization characteristics due to ionospheric scintillation. (*a*) "Type C" scintillation. (*b*) "Type S" scintillation. (upper) Amplitude of vertical polarization component. (middle) Relative phase difference between the two orthogonal components. (lower) Scattergram of both amplitudes.

polarization (LHCP)) is estimated by

$$P_x = \frac{1 + a^2 - 2a \cos \Delta\Theta}{1 + a^2 + 2a \cos \Delta\Theta} \tag{3}$$

P_x Power of cross-polarization component (LHCP) relative to the power of copolarization component (RHCP)

$a = |E_V/E_H|$

$\Delta\Theta = \angle E_V - \angle E_H - (\overline{\angle E_V - \angle E_H})$

Figures 13*a* and 13*b* show the amplitude of the vertically polarized component, phase difference, and scattergram between amplitudes of vertically and horizontally polarized components for type C and type S scintillations, respectively. In both cases, the deviation of amplitudes between the two components was smaller than 0.2 dB and the fluctuation of phase difference was smaller than 3°. From equation (3), the cross-polarization component, even for fairly large scintillations, was not more than −30 dB relative to the copolarization component. It is concluded that the depolarization for circularly polarized waves at gigahertz frequencies due to ionospheric scintillation is expected to be negligible.

4. CONCLUDING REMARKS

Experimental results on 1.5-GHz ionospheric scintillations in the mid-latitude region have been described. In the 13-month-long observations at an elevation angle of 17.3°, the following results were obtained:

1. Two type of scintillations were observed, one (type C) lasting for a long period commonly seen in literatures, and the other of a spike type (type S). The type S scintillation has only one or two fairly large signal fades in one event. This type of scintillation seems to be caused by a small scale irregularities such as blobs generated in the ionosphere.

2. Onset time of scintillation had two peaks in a day, namely, from 0900 to 1500 hours and from 2000 to 0100 hours local time, with the latter peak dominant for the type S scintillations.

3. With regard to seasonal variation of scintillation occurrence, a number of weak scintillation ap-

peared in early summer while a few severe scintillation occurred in the equinoctial months.

4. Even in the strong scintillation whose amplitude follows the Rayleigh distribution, the power spectrum of ionospheric scintillation shows a marked power-law form of f^{-3}. The fluctuation period of such severe scintillation becomes longer with time.

5. The cross-polarization component for a circularly polarized wave caused by ionospheric irregularities was smaller than -30 dB even for fairly large scintillation of both type C and type S. Therefore, depolarization due to ionospheric scintillation is expected to be negligible at L band frequencies.

It seems important to ascertain whether the above-mentioned characteristics of L band scintillation observed in the middle latitude region can be generally seen at other regions and at different frequencies, especially for type S scintillations.

Acknowledgments. The authors would like to express their sincere thanks to H. Kaji, K. Nosaka, and A. Ogawa, KDD R & D Labs for their continuous encouragement. Thanks are also due to the members of the Yamaguchi Satellite Communication Center in KDD for their helpful cooperations.

REFERENCES

Aarons, J., Global morphology of ionospheric scintillations, *Proc. IEEE*, *70*(4), 360–378, 1982.

Aarons, J., and H. E. Whitney, Ionospheric scintillations at 136 MHz for a synchronous satallite, *Planet. Space Sci.*, *16*, 21–28, 1968.

Basu, S., S. Basu, and B. K. Khan, Model of scintillations from in situ measurements, *Radio Sci.*, *11*(10), 821–832, 1976.

Basu, S., S. Basu, J. P. McClure, W. B. Hanson, and H. E. Whitney, High resolution topside in situ data of electron densities and VHF/GHz scintillations in the equatorial region, *J. Geophys. Res.*, *88*(A1), 403–415, 1983.

Crane, R. K., Ionospheric scintillation, *Proc. IEEE*, *65*(2), 180–199, 1977.

Davies, K., and J. D. Whitehead, A radio lens in the ionosphere, *J. Atmos. Terr. Phys.*, *34*, 927–939, 1979.

Fang, D. J., and C. H. Liu, A morphological study of gigahertz equatorial scintillations in the Asian region, *Radio Sci.*, *18*, 241–252, 1983.

Franke, S. J., and C. H. Liu, Observations and modeling of multifrequency VHF and GHz scintillation in the equatorial region, *J. Geophys. Res.*, *88*(A9), 7075–7085, 1983.

Fremouw, E. J., R. C. Livingston, and D. A. Miller, On the statistics of scintillating signals, *J. Atmos. Terr. Phys.*, *42*, 717–731, 1980.

Fujita, M., T. Ogawa, and K. Koide, 1.7 GHz scintillation measurements at mid-latitude using a geostationary satellite beacon, *J. Atmos. Terr. Phys.*, *40*, 963–968, 1978.

Hajkowicz, L. A., E. N. Bramley, and R. Browning, Drift analysis of random and quasiperiodic scintillations in the ionosphere, *J. Atmos. Terr. Phys.*, *43*, 723–733, 1981.

Karasawa, Y., and K. Yasukawa, Gradual change of power spectrum of ionospheric scintillation, *Trans. IECE Jpn.*, *E*(64-E), 606–607, 1981.

Karasawa, Y., and K. Yasukawa, Tropospheric scintillation in a low elevation angle at 11 GHz, *Natl. Conf. IECE Jpn.*, 687, 1983.

Moriya, Y., and H. Sakurada, Ionospheric scintillation shown in the MARISAT Satellite, *Trans. IECE Jpn.*, *J66-B*(11), 1430–1431, 1983.

Rufenach, C. L., Ionospheric scintillation by a random phase screen spectral approach, *Radio Sci.*, *10*, 155–161, 1975.

Slack, F. F., Quasiperiodic scintillation in the ionosphere, *J. Atmos. Terr. Phys.*, *34*, 927–939, 1972.

Taur, R. R., Ionospheric scintillations at 4 and 6 GHz, *COMSAT Tech. Rev.*, *3*(1), 145–163, 1973.

Taur, R. R., Simultaneous 1.5- and 4-GHz ionospheric scintillation measurement, *Radio Sci.*, *11*(12), 1029–1036, 1976.

Tyagi, T. R., K. C. Yeh, and A. Taurianen, The electron content and its variations at Natal, Brazil, *J. Geophys. Res.*, *87*(A4), 2525–2532, 1982.

Yeh, K. C., and C. H. Liu, Radio wave scintillations in the ionosphere, *Proc. IEEE*, *70*(4), 324–360, 1982.

Y. Karasawa, M. Yamada, and K. Yasukawa, Research and Development Laboratories, Kokusai Denshin Denwa Co., Ltd., 2-1-23, Nakameguro, Meguro-ku, Tokyo 153, Japan.